TOXICOLOGY AND APPLIED PHARMACOLOGY **148,** 35–45 (1998)
ARTICLE NO. TO978316

Toxicity of Atractyloside in Precision-Cut Rat and Porcine Renal and Hepatic Tissue Slices

David K. Obatomi,*,† Stephen Brant,† Vethanayagam Anthonypillai,† and Peter H. Bach‡,[1]

**Department of Biochemistry, Faculty of Medical Sciences, University of Jos, P.M.B. 2084, Jos, Nigeria; †Faculty of Science and Health, University of East London, Romford Road London E15 4LZ, United Kingdom; and ‡BioTechnologic Ltd., Khaya Lami House, Castle Road, Horsell, Woking, Surrey GU21 4EU, United Kingdom*

Received March 3, 1997; accepted September 21, 1997

Toxicity of Atractyloside in Precision-Cut Rat and Porcine Renal and Hepatic Tissue Slices. Obatomi, D. K., Brant, S., Anthonypillai, V., and Bach, P. H. (1998). *Toxicol. Appl. Pharmacol.* **148, 35–45.**

Atractyloside (ATR) causes acute fatal renal and hepatic necrosis in animals and humans. Precision-cut renal cortical and hepatic slices (200 ± 15 μm) from adult male Wistar rat and domestic pigs, incubated with ATR (0.2–2.0 mM) for 3 h at 37°C, inhibited pyruvate-stimulated gluconeogenesis in a concentration- and time-dependent manner. *p*-Aminohippurate accumulation was significantly inhibited in both rat and pig renal cortical slices from 0.2 mM ATR ($p < 0.05$). There was a small decrease in mitochondrial reduction of 3-(4,5-dimethylthiazol-2-yl)-2,5-diphenyltetrazolium to formazan in both rat and pig kidney slices, which was significant at ≥2 mM, but no changes in liver slices from either species. However, cellular ATP was significantly depleted at ≥0.2 mM ATR in kidney and in liver slices from both species. ATR also caused a marked leakage of lactate dehydrogenase and alkaline phosphatase from both pig and rat kidney slices at all concentrations, but only lactate dehydrogenase was significantly elevated in liver slices from both species. ATR ≥ 0.5 mM caused a significant increase in lipid peroxidation, but only in liver slices of both species, and ≥0.2 mM ATR caused a marked depletion of reduced glutathione and significant increase in oxidized glutathione in both kidney and liver slices of both species. However, GSH to GSSG ratio was only significantly altered in the liver slices, indicating that oxidative stress may be the cause of toxicity in this organ. Both rat and pig tissue slices from the same organ responded similarly to ATR, although their basal biochemistry was different. ATR toxicity to both kidney and liver showed similar patterns but it appears that the mechanisms of toxicity are different. While cytotoxicity of ATR in kidney is only accompanied with GSH depletion, that of the liver is linked to both lipid peroxidation and GSH depletion. Striated muscle slices from both species were not affected by the highest ATR concentration. This further strengthens the argument that the molecular basis of ATR, target selective toxicity, is not a measure of the interaction between ATR and mitochondria and that other factors such as selective uptake are involved. Precision-cut tissue slices show organ-specific toxicity in kidney and liver from both rat and pig and suggest different mechanisms of injury for each organ. © 1998 Academic Press

Key Words: **atractyloside; diterpenoid; target cell toxicity; renal and hepatic precision-cut tissue slices; cytotoxicity; rat; pig.**

Throughout Africa and the Mediterranean, many of the plants used in ethnomedicines and herbal and alternative medications contain atractyloside (ATR),[2] a diterpenoid glycoside (Fig. 1) that causes acute proximal tubule necrosis leading to renal failure and death in humans (Wainwright *et al.*, 1977; Bhoola, 1983; Caravaca-Magarinos *et al.*, 1985; Georgiou *et al.*, 1988) and domestic animals foraging on ATR-containing plants (Stuart *et al.*, 1981; Hatch *et al.*, 1982; Martin *et al.*, 1986). ATR also causes acute centrilobular hepatic necrosis (Stuart *et al.*, 1981; Hatch *et al.*, 1982; Bhoola, 1983; Georgiou *et al.*, 1988). ATR is known to inhibit mitochondrial respiration (Allman *et al.*, 1967; Luciani *et al.*, 1978), but the mechanism of target cell injury specifically for the proximal tubule and the centrilobular region within the liver are not well understood (Obatomi and Bach, 1997). Thus, despite significant human exposure and many reported deaths (Bhoola, 1983; Hutchings and Terblanche, 1989), there is no rational approach to limit or prevent ATR toxicity.

Recent findings from our laboratory (Obatomi and Bach, 1996a) have shown that cell lines derived from proximal tubules and freshly isolated proximal tubule fragments (but not cells from other regions of the kidney) are sensitive to the toxic effect of ATR. This suggests a possibility to mimic *in vivo* effects of ATR *in vitro.* In addition, we have shown that ATR inhibited respiration similarly for both isolated liver and kidney mitochondria (Obatomi and Bach, 1996b). While cultured cells (Obatomi and Bach, 1996a) and isolated mitochondria (Obatomi and Bach, 1996b) help us understand more about the

[1] To whom all correspondence and reprint requests should be addressed at BioTechnologic Ltd., Khaya Lami House, Castle Rd., Horsell, Woking, Surrey GU21 4EU, UK. Fax: 44 +(0)1483 773601. E-mail: PeterHBach@Compuserve.com.

[2] Abbreviations used: ALP, alkaline phosphatase; ATR, atractyloside; LDH, lactate dehydrogenase; MDA, malondialdehyde; MTT, 3-(4,5-dimethylthiazol-2-yl)-2,5-diphenyltetrazolium bromide; PAH, *p*-aminohippurate.

0041-008X/98 $25.00

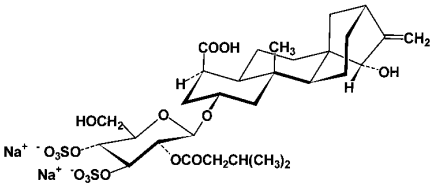

Atractyloside

FIG. 1. The structure of atractyloside.

effects of ATR, these systems cannot provide an insight into the molecular basis of target cell injury or allow kidney and liver sensitivity to be contrasted or any interspecies comparisons to be made. We have therefore used ''precision-cut'' tissue slices (Brendel *et al.,* 1993; Bach *et al.,* 1996a,b; Gandolfi *et al.,* 1996), which offer the potential to compare the target cell toxicity of ATR in renal and hepatic tissues from different species. The advantages of this *in vitro* system is that several parameters can be determined simultaneously in slices prepared from same animals and incubated under identical conditions, which has a greater utility for mechanistic studies (Brendel *et al.,* 1993; Bach *et al.,* 1996a,b; Gandolfi *et al.,* 1996). Thus there would be the potential to understand the mechanism of ATR toxicity *in vitro,* which would provide an insight into the possible ways of modulating its toxic effects. This is the first attempt to reproduce nephro- and hepatotoxicity using a higher order *in vitro* systems, where the cellular architecture maintains the heterogeneity of the intact organ. The objective of this study was to investigate the appropriateness of precision-cut slices as an *in vitro* model in assessing toxic events following exposure to ATR. To achieve this goal we have assessed the effects of ATR in kidney and liver slices from the rat and pig where *in vivo* data are available (Carpenedo *et al.,* 1974; Bhoola, 1983; Bye, 1991; Stuart *et al.,* 1981; Hatch *et al.,* 1982) and functional and biochemical changes can be compared. We also selected striated muscle as a source of cells that had high mitochondrial activity but was not reported to be a target tissue. This has allowed us to determine the direct effects of ATR on specific cell types in each tissue and to compare its effects on renal and hepatic function in both species.

MATERIALS AND METHODS

Reagents. All chemicals were of analytical grade (Sigma Chemical Company, Poole, Dorset, UK) unless otherwise stated.

Animals and harvesting of tissues. Male adult domestic pigs, moved straight from farms to a local abattoir for slaughter, were used as sources of fresh tissue. One kidney (usually the right), a lobe of liver, and a portion of pericardium tissue were removed within 5 min of slaughter, and the tissues were transported to the laboratory in ice-cold Krebs–Hepes buffer. Tissues were cored for slicing within 25–30 min of harvesting.

Male Wistar rats (200–220 g) were obtained from Charles River (Kent, UK) and housed under a controlled ambient temperature (21–23°C) and 12-h light-dark cycle (starting at 0600 hour). The animals were acclimatized to housing conditions for at least 3 days prior to use and were maintained on standard laboratory rat chow (Laboratory Diet No. 1, Spratts, Barking, Essex, UK) and tap water *ad libitum.* Individual rats were euthanized by cervical dislocation, and the liver, kidney, and a portion from the pericardium tissue were quickly excised and immediately placed in an ice-cold pregassed (95% O_2: 5% CO_2) rinse medium (Krebs–Hepes buffer, pH 7.4).

Slice preparation. Different areas of the rat and pig liver lobes were cored parallel with, but excluding, the major blood vessels, with a motorized tissue coring press equipped with an 8-mm diameter stainless steel corer (Alabama Research and Development Corp., Munford, AL). Rat kidneys were decapsulated and cylindrical cores (8 mm in diameter) made perpendicular to the cortico-papillary axis. Pig renal cortex was similarly cored. Tissue cores (8 mm in diameter) were similarly prepared from a longitudinal section of the striated muscle from the pericardium. The cores were then placed in ice-cold Krebs–Hepes buffer and transferred one at a time to a Krumdieck tissue slicer (Krumdieck *et al.,* 1980).

Tissue slices (200 ± 15 μm) were prepared in ice-cold sterile phosphate-buffered saline (PBS) and 0.1% (w/v) agarose (low gelling temperature). Slices were collected and placed individually in a 24-well plate, containing 1 ml serum-free, phenol red-free Dulbecco modified Eagle's nutrient mixture:F12 Ham (DMEM/F12) and were preincubated on an orbital shaker (Bellco Biotechnology, Vineland, NJ) in a humidified incubator at 37°C for 1 h to allow slices to stabilize (Obatomi *et al.,* 1997).

Slice viability assessment. After preincubation, representative slices from each preparation were assessed for viability after a short incubation with 200 μg/ml ethidium bromide and 5 μg/ml fluorescein diacetate in PBS (Edindin, 1970). Slices were observed under a Leitz Dialux 20 (Leica UK Ltd., Milton Keynes) microscope (390–490 nm excitation and 510–515 nm emission). This provides a rapid qualitative assessment of viable cells (the cytoplasm of which fluoresce bright green), whereas the nuclei of nonviable cells fluoresce red.

Incubation of slices. Following the 1-h period of preincubation, the medium was removed and replaced with 1 ml of fresh medium containing ATR (0–2.0 mM) and slices were incubated for 3 h at 37°C on a rocker platform rotated at approximately 3 rpm. At the end of the incubation periods, the medium was removed and used to assay LDH and ALP leakage. MTT reduction was assessed in one series of slices immediately, and lipid peroxidation, reduced (GSH) and oxidized (GSSG) glutathione, and ATP contents were measured in another series of slices as described below. All incubation of slices from both rat and pig tissues were carried out under identical conditions.

Enzyme leakage. LDH and ALP activities in the incubation medium were measured by the methods described by Obatomi and Plummer (1995). Baseline data are expressed as micromoles per minute per milligram of protein. Total enzyme activity was determined using slices disrupted by addition of 1% (w/v) Triton X-100.

Mitochondria viability. Slices were incubated with 1.21 mM MTT solution dissolved in PBS (Mosbann, 1978). After 40 min at 37°C, the MTT solution was removed, slices were rinsed with PBS, and the formazan product was extracted in 1 ml isopropanol and absorbance was measured at 570 nm. MTT absorbance was related to the protein concentration that was assayed after extraction with isopropanol and expressed as percentage of control values.

Assessment of ATP content. ATP was quantified in slices by using the bioluminescent reaction catalyzed by luciferase (DeLuca and McElroy, 1978). After incubation of slices with ATR, slices were homogenized in 1 ml 0.398 M TCA using an ultra Turrax T8 homogenizer (IKA Labortechnik, Janke & Kunkel GmbH & Co., Germany), the precipitate was removed by centrifugation at 4000 rpm for 5 min, and 10 μl of the supernatant was added to 2 ml of 25 mM HEPES buffer (pH 7.75). The luciferin–luciferase solution (100 μl of 5 mg/ml) was added to 200 μl of each sample or standard in a luminometer cuvette. Bioluminescence was then quantified in a luminescence photometer (1251 Luminometer, LKB Wallac, Finland). ATP content was determined from the standard curve (1–200 ng/ml) and expressed as nanograms ATP per milligram of protein.

TABLE 1
Summary of Control Data

Parameter	Liver		Kidney	
	Pig	Rat	Pig	Rat
Formazan (Abs_{570}/mg protein)	0.185 ± 0.012	0.16 ± 0.023	0.482 ± 0.018†	0.50 ± 0.130†
ATP (ng/mg protein)	12.9 ± 0.96	13.2 ± 0.93	9.54 ± 0.61†	11.6 ± 0.32*
ALP (nmol/min/mg protein)	0.119 ± 0.014	0.0267 ± 0.016**	0.210 ± 0.050†	0.109 ± 0.0036**·†
LDH (nmol/min/mg protein)	0.027 ± 0.013	0.051 ± 0.05**	0.048 ± 0.022†	0.029 ± 0.002**·†
Lipid peroxidation (nmol/mg protein)	0.70 ± 0.20	1.55 ± 0.28**	0.50 ± 0.10	3.12 ± 0.51**·†
GSH (ng/mg protein)	381.4 ± 29.7	301.3 ± 23.1	232.4 ± 19.7††	178.4 ± 16.6††
GSSG (ng/mg protein)	15.7 ± 1.8	16.2 ± 2.05	12.9 ± 2.33	9.91 ± 1.42*
Glucose (mg/g tissue)[a]	25.7 ± 3.17	24.8 ± 3.73	5.51 ± 0.57**·††	1.653 ± 0.297†††
PAH s/m ratio[a]	ND	ND	15.1 ± 3.61	11.2 ± 0.62

Note. Each value is the mean ± SE of three experiments in which four slices were used for each parameter. Slices of 200 ± 15 μm were incubated as described in the Materials and Methods section for 3 h at 37°C in the absence of atractyloside. ND, not determined; *$p < 0.05$, **$p < 0.01$, ***$p < 0.001$, significantly different between the same tissue in different species; †$p < 0.05$, ††$p < 0.01$, †††$p < 0.001$, significantly different between the different tissues in the same species.

[a] Values obtained after 60-min incubation.

Determination of malondialdehyde. Lipid peroxidation was monitored by the production of malondialdehyde (MDA) by using the thiobarbituric acid (TBA) assay (Burge and Aust, 1978). After incubation, the slices were removed, weighed, and homogenized in 3 ml of the TBA reagent (0.026 M thiobarbituric acid, 0.92 M trichloroacetic acid, and 0.25 M HCl). The homogenate was heated at 100°C for 15 min and cooled. The precipitate was removed by centrifugation at 3000 rpm for 10 min, and the absorbance of the supernatant was determined at 535 nm. The MDA concentration of the sample was calculated using an extinction coefficient of 1.56×10^5 M^{-1} cm^{-1} (Burge and Aust, 1978).

Glutathione content of slices. Both oxidized (GSSG) and reduced (GSH) forms of glutathione in slices were measured using a modified method of Hissin and Hilf (1976). Slices were deproteinized in 0.5 ml trichloroacetic acid (0.398 M). Samples were then centrifuged for 10 min at 3000 rpm. For GSH assay, 75 μl of the supernatant was removed and mixed with 2775 μl of 0.1 M phosphate/0.005 M EDTA buffer (pH 8.0); 150 μl of *o*-phthaldiadehyde solution (74.6 mM) was added, mixed, and incubated for 25 min at room temperature. For GSSG assay, 0.25 ml of the supernatant was removed, mixed with 100 μl *N*-ethylmaleimide (40 mM), and incubated at room temperature for 30 min. To this was added 2.25 ml NaOH (0.1 M), and 75 μl of this mixture was then added to 2775 μl of NaOH (0.1 M) and 150 μl of *o*-phthaldialdehyde solution (74.6 mM), which was mixed and incubated for 25 min. Fluorescence was measured (LS-5L luminescence spectrometer, Perkin-Elmer) at excitation of 350 nm and emission of 420 nm. Both GSH and GSSG were expressed as nanograms per milligram of slice protein, based on a standard curve.

Evaluation of gluconeogenesis. After incubation with ATR for 3 h, slices were rinsed with PBS and further incubated in glucose-free Krebs Henseleit solution (pH 7.4) containing pyruvate (10 mM) for 60 mins in order to stimulate gluconeogenesis (Roobol and Alleyne, 1974). At the end of the incubation period, slices were removed, blotted, and weighed. Aliquots of the incubation medium were assessed for glucose by the glucose oxidase and peroxidase assay (Plummer, 1987) and expressed as milligrams glucose per grams of tissue wet weight per 60-min incubation with pyruvate. However, because of the quantitative difference in the control level of glucose production in the kidney and liver slices (Table 1), the result was expressed as percentage of control for comparative purposes.

Organic ion accumulation. PAH accumulation by renal cortical slices was determined according to the method of Smith *et al.* (1944). After 3-h incubation with ATR, slices were further incubated in 4 ml medium containing 0.074 mM PAH (Fujimoto and Fujita, 1982) at 37°C for 30 min. At the end of incubation, slices were removed, blotted, weighed, homogenized in (10 ml/100 mg tissue) 0.184 M trichloroacetic acid, and centrifuged at 3000 rpm for 10 min. A 1-ml aliquot of the incubation medium was treated similarly. The supernatant was assayed for PAH by diazotization. Renal accumulation of PAH was expressed as the slice-to-medium (*S*/*M*) ratio, where *S* represents the concentration of PAH per gram tissue in the slice, and *M* represents PAH per milliliter in medium. Data were presented as percentage of the control accumulation at each time point for ease of comparison.

Protein assays. Slices were dissolved in 1.0 ml of 0.5 M NaOH for 24 h, and protein content was assessed by the Coomassie Brilliant G method (Read and Northcote, 1981) using bovine serum albumin as a standard. Protein concentrations were used to normalize data obtained in all other assays.

Statistical analysis. Experimental data in quadruplicate were obtained from at least three separate experiments. Results are expressed as means ± SE. Statistical evaluation of data was performed by two-way analysis of variance. Differences between the means of experimental and control groups within same species or between species were made using the least significant difference test with $P < 0.05$ considered significant.

RESULTS

Baseline Data in Untreated Tissue Slices

Table 1 provides a direct comparison of control data of all the parameters measured after 3-h incubation for both rat and pig. MTT reduction was higher in the kidney slices of both rat and pig than in the liver slices, but there was no interspecies difference. ATP content was significantly ($p < 0.05$) higher in the liver than the kidney of the pig; the latter being significantly ($p < 0.05$) lower in the pig than the rat. ALP and LDH leakage from the kidney slices of both rat and pig were significantly greater ($p < 0.05$) than those of liver slices. The leakage of these enzymes was significantly higher ($p < 0.01$) in the liver slices of rat compared to those of the pig. There was, however, less leakage from rat kidney slices compared to those of the pig. There was less lipid peroxidation in pig tissues than in the rat. The rat showed greater

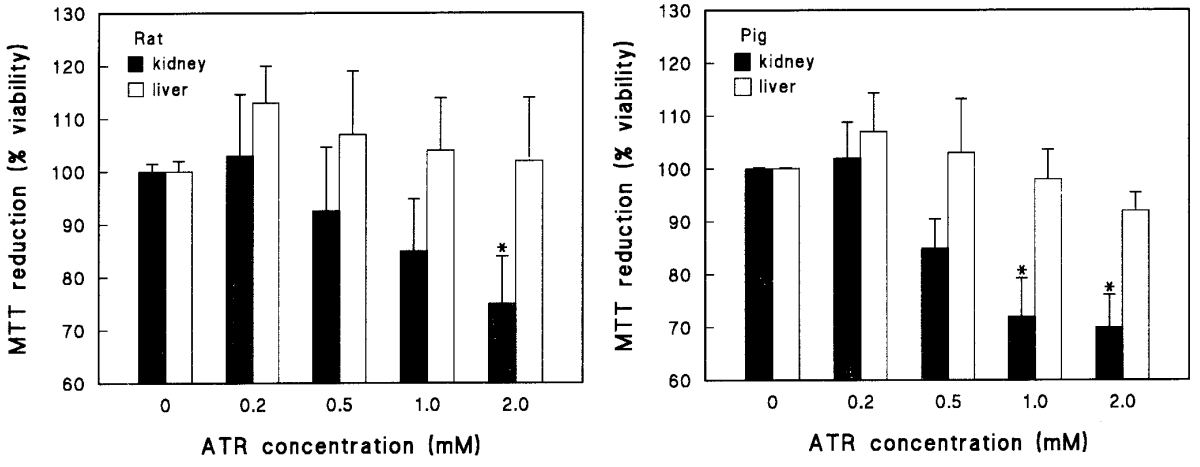

FIG. 2. MTT reduction to formazan in liver and kidney slices from both rat and pig exposed to ATR. The data are expressed as a percentage of the mean absorbance of untreated slices incubated for same time intervals and are presented as the means ± SE from three experiments in quadruplicate. Statistically significant difference between the ATR exposed versus the control groups are indicated as $*p < 0.01$.

lipid peroxidation in the kidney slices than the liver. Intracellular GSH level was significantly ($p < 0.05$) higher in the kidney and liver slices of the pig than the corresponding organ in the rat. However, there was no significant difference in GSH levels in the liver and kidney of the pig compared to the corresponding organs of the rat. The GSSG levels in the rat liver was significantly ($p < 0.05$) higher than that of the kidney but the levels in the liver were of the same magnitude in the two species. Gluconeogenic capacity of the liver slices in both rat and pig was at least fivefold higher than that of kidney slices. Accumulation of PAH followed a similar pattern in both rat and pig kidney slices and the ratio were of the same magnitude.

Effects of ATR on MTT Reduction

The cytotoxic effect of ATR on liver and kidney slices as characterized by the MTT assay shows a small dose-related decrease in viability that was significant ($p < 0.05$) at concentrations ≥1.0 and ≥2.0 mM in rat and porcine kidney slices, respectively, while there were no significant changes in liver slices from either species (Fig. 2).

Effects of ATR on Intracellular ATP Content

ATR caused a marked and statistically significant concentration-dependent decrease in ATP content in both liver and kidney slices and from both species (Fig. 3).

Effects of ATR on Enzyme Leakage

Figures 4 and 5 show the concentration-related, significant leakage of ALP and LDH from rat (≥0.2 mM) and porcine (≥0.5 mM) kidney slices exposed to ATR. LDH leakage was significantly elevated in porcine liver slices at ATR concen-

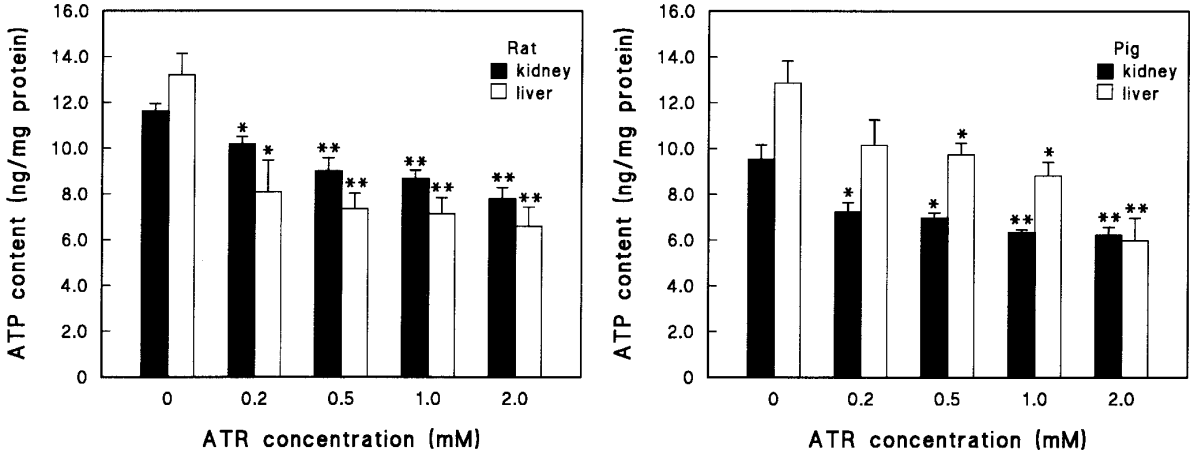

FIG. 3. Effect of ATR on intracellular ATP content in rat and porcine liver and renal cortical slices. Values given are the means ± SE of three separate experiments representing four slices. $*p < 0.05$, $**p < 0.01$ compared to control groups.

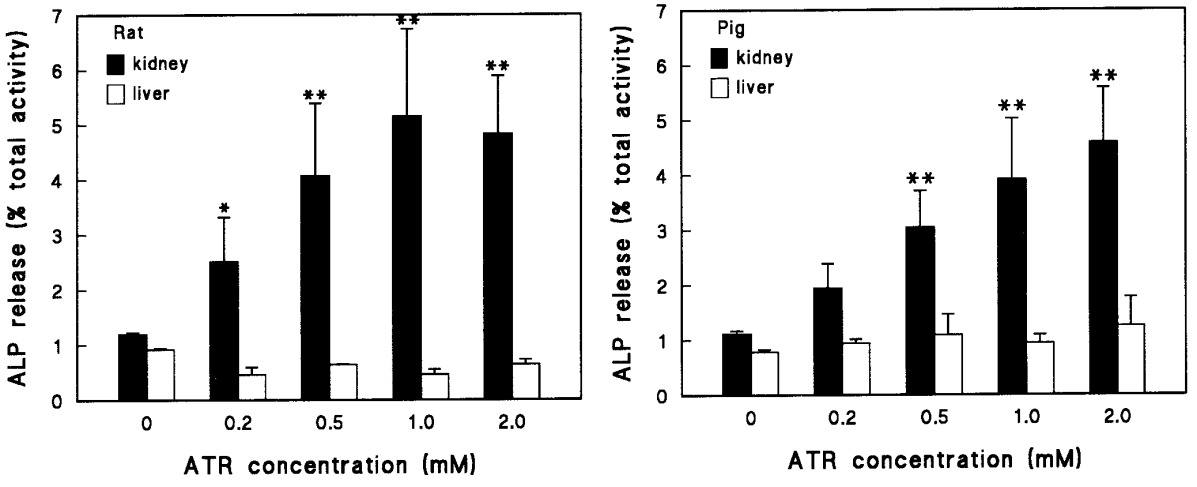

FIG. 4. ALP leakage from rat and porcine liver and renal cortical slices exposed to ATR. The data are expressed as percentage of total amount of ALP in tissue and medium and presented as the means ± SE ($n = 3$ of 4 slices; $*p < 0.05$, $**p < 0.01$, $***p < 0.001$ compared to control groups).

trations ≥ 0.5 mM and was dose related while a significant leakage of LDH from rat liver slices at 0.2 mM ATR was not present at higher concentrations. ALP was not changed by any ATR concentration in either porcine and rat hepatic slices. Kidneys from both rat and pig show equal sensitivity to ATR as assessed by the release of ALP. There was a dose-related increase of LDH following ATR treatment in pig tissues, but there were relatively little and insignificant changes in the leakage of this enzyme in rat liver slices.

Effects of ATR on Lipid Peroxidation and Glutathione Levels

Lipid peroxidation, as quantified by MDA production, was significantly elevated in porcine and rat liver slices at ATR concentration ≥0.2 and ≥0.5 mM, respectively (Fig. 6), as compared to kidney slices, where there were no significant changes at any concentration of ATR. There was higher basal peroxidation in rat than in the porcine kidney slices. However, ATR induced a dose-dependent depletion of intracellular GSH levels in both pig and rat kidney and liver slices. GSSG levels were marginally increased in the kidney in a dose-dependent manner while the increase was statistically significant in the liver. However, the GSH to GSSG ratio showed a significant decrease in the liver but not in the kidney (Fig. 7).

Effects of ATR on Gluconeogenesis

Pyruvate-stimulated gluconeogenesis was inhibited in a concentration- and time-dependent manner in both liver and kidney slices (Fig. 7). Although glucose production in the untreated kidney and liver slices of rat and pig showed a wide variation (Table 1), the response to ATR was however very similar (Fig. 8). The inhibitory effect of ATR follows a similar pattern in both the kidney and liver slices of both species.

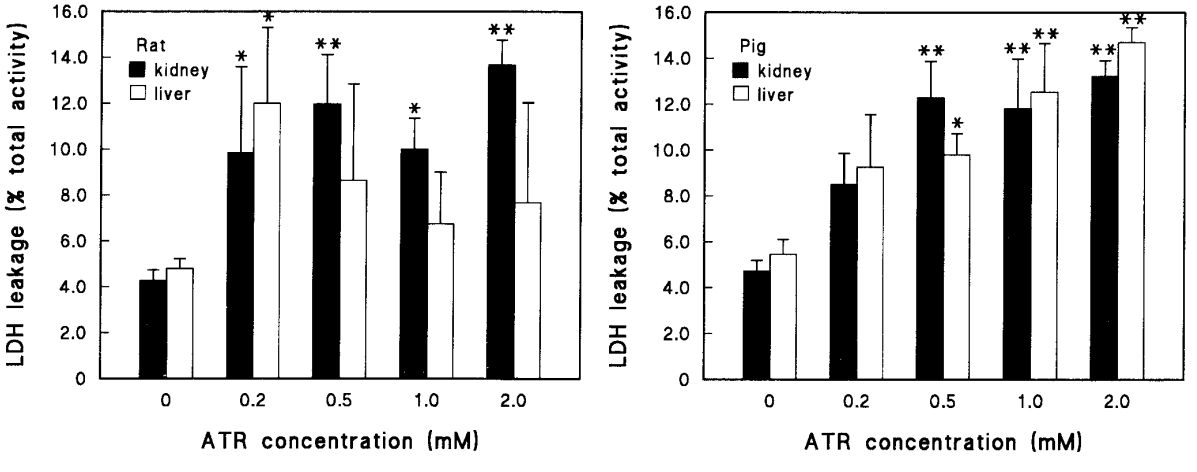

FIG. 5. LDH leakage from rat and porcine liver and renal cortical slices exposed to ATR. The data are expressed as percentage of total amount of LDH in tissue and medium and presented as the means ± SE ($n = 3$ of 4 slices; $*p < 0.05$, $**p < 0.01$ compared to control groups).

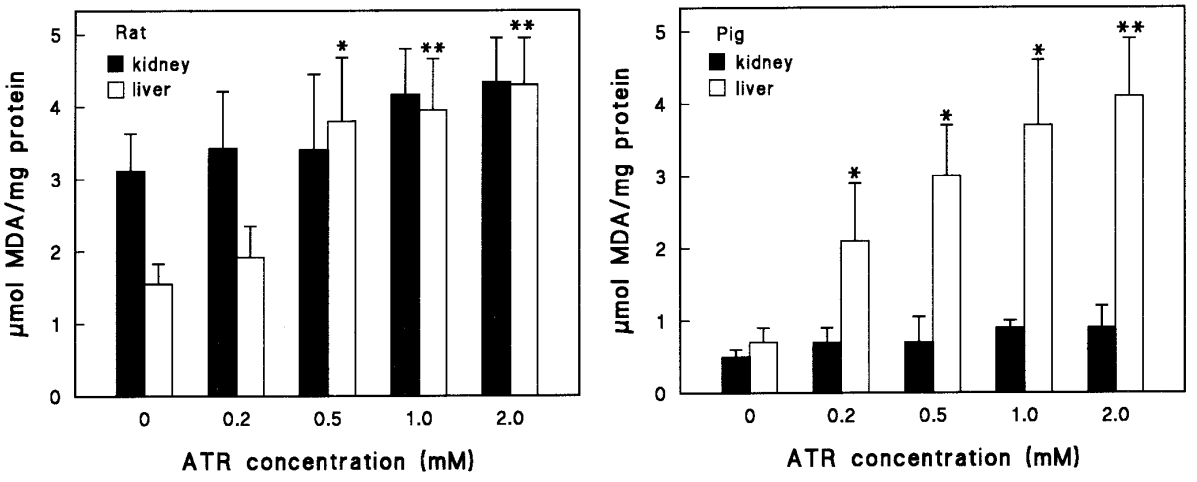

FIG. 6. Effects of ATR on MDA production in rat and porcine liver and renal cortical slices. MDA production was measured by the thiobarbituric acid assay. The data are presented as means ± SE ($n = 3$ of 4 slices). Statistically significant differences between treated and control groups are indicated as $*p < 0.01$, $**p < 0.001$.

Gluconeogenesis was only decreased in the presence of ATR concentration ≥0.5 mM. Endogenous gluconeogenesis (in the absence of exogenous pyruvate) was also inhibited to the same extent by ATR, an indication that inhibition of pyruvate uptake is not the cause of ATR-induced decrease of gluconeogenesis (data not shown).

Effects of ATR on PAH Accumulation

PAH accumulation by renal cortical slices was very sensitive to ATR with PAH accumulation significantly decreased at concentration as low as 0.2 mM in rat (Fig. 9). The reduction in PAH accumulation was concentration- and time-dependent. PAH accumulation in untreated slices increased over the period of incubation from 10.2 ± 1.0; 12.8 ± 2.74 at 30 min rising to 11.2 ± 0.62; 15.1 ± 3.61 at 60 min in rat and pig, respectively.

Effects of ATR on Nontarget Tissue

A summary of the effect of ATR on striated muscle slices of rat and pig and characterized by four toxicity profiles is shown in Table 2. There were no significant alterations in any of these parameters even at the highest dose of ATR when compared to untreated tissue.

DISCUSSION

Fatal liver and kidney necrosis following the ingestion of herbal remedies containing atractyloside is increasingly com-

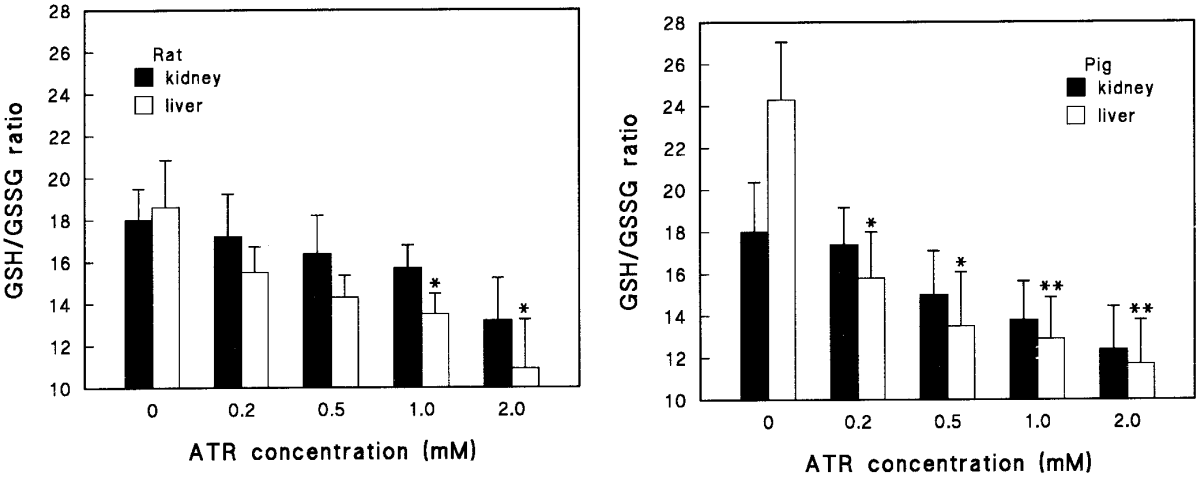

FIG. 7. Effects of different ATR concentrations on GSH to GSSG ratio in rat and porcine liver and renal cortical slices. The data are presented as means ± SE ($n = 3$ of 4 slices). Significantly different from corresponding control, $*p < 0.01$, $**p < 0.001$).

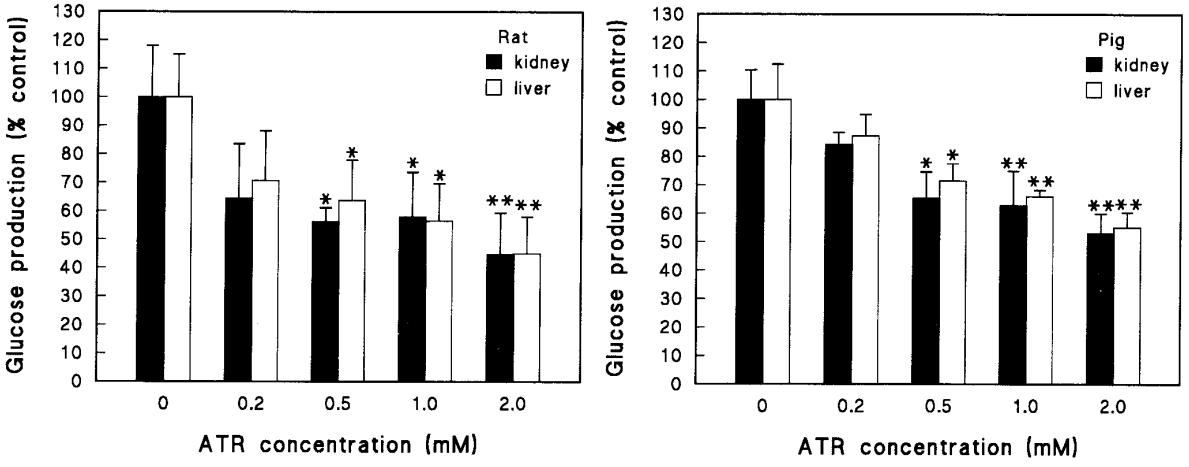

FIG. 8. Effects of different ATR concentrations on pyruvate-stimulated gluconeogenesis in rat and porcine liver and renal cortical slices. Pyruvate-stimulated gluconeogenesis was measured as glucose production after a subsequent 1-h incubation in pyruvate containing Atr-free medium. Data are presented as percentage of control glucose production, means ± SE ($n = 3$ of 4 slices). Glucose production after incubation with Atr are significantly different compared to corresponding control values, $*p < 0.05$, $**p < 0.01$.

mon in Africa and along the Mediterranean. Each year a significant number of children and adults die after consuming ATR-containing plants or their decoctions (Wainwright *et al.*, 1977; Bhoola, 1983; Hutchings and Terblanche, 1989; Georgiou *et al.*, 1988), and there are also reported cases of livestock poisoning (Roeder *et al.*, 1994; Schteingart and Pomilio, 1984) as a result of grazing on ATR-containing plants.

There is also some evidence of species- and strain-related differences for ATR target organ toxicity (Bhoola, 1983; Luciani *et al.*, 1978; Carpenedo *et al.*, 1974). For instance, rabbits and guinea pigs do not develop renal necrosis following doses of ATR that are nephrotoxic for rats (Carpenedo *et al.*, 1974; Wainwright *et al.*, 1977; Georgiou *et al.*, 1988). There may also be strain differences as male albino rats (strain not defined) tolerated up to 200 mg/kg ATR, whereas male Wistar rats died within 8 h after receiving 60 mg/kg ATR. In addition, while both liver and kidney are targets for ATR (Bhoola, 1983; Caravaca-Magarinos *et al.*, 1985), published data suggest that the kidney is more often adversely affected *in vivo* (Bhoola, 1983; Carpenedo *et al.*, 1974).

We have assessed the response of kidney and liver to ATR in order to elucidate more about the probable mechanism of toxicity. These studies have used the major target organs from the rat and pig. The choice of the pig tissue is because this species is sensitive to atractyloside *in vivo* (Stuart *et al.*, 1981; Hatch *et al.*, 1982), and the fact that there are marked morphological and functional similarities between porcine and human kidney and liver (Mount and Ingram, 1971; Douglas,

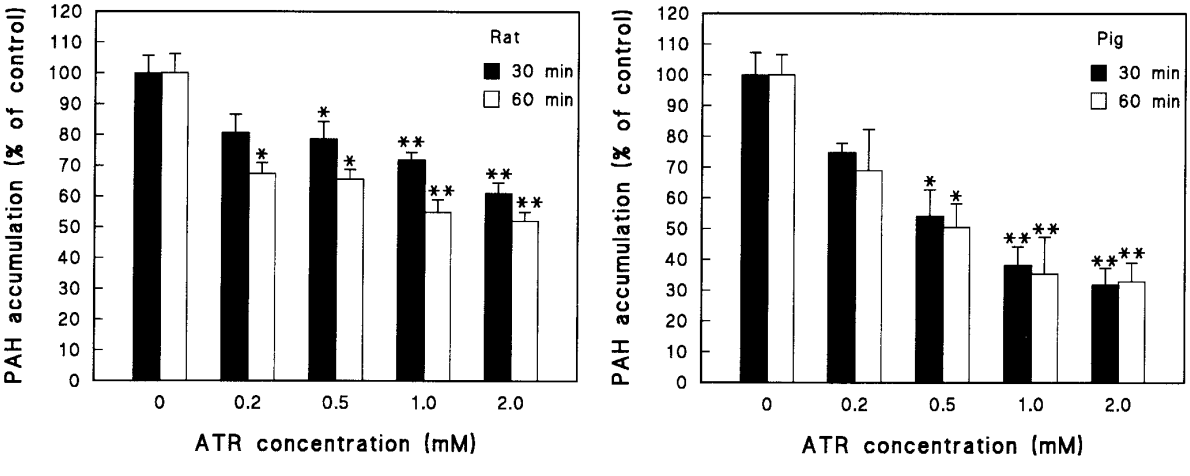

FIG. 9. Time- and dose-dependent effect of different ATR concentrations on PAH accumulation in rat renal cortical slices. PAH accumulation was calculated as slice to medium (S/M) concentration ratio but presented as percentage of the control accumulation in slices, means ± SE ($n = 3$ of 4 slices and as compared to corresponding control values, $*p < 0.05$, $**p < 0.001$).

TABLE 2
Effect of ATR on Striated Muscle Slices in Rat and Pig Tissue

	ATR concentration			
	Rat		Pig	
Parameters	0 mM	2 mM	0 mM	2 mM
MTT (% viability)	100.0 ± 1.2	102.3 ± 2.7	100 ± 0.9	96.4 ± 3.2
LDH (% total activity)	6.35 ± 1.43	7.10 ± 2.1	5.90 ± 2.3	6.2 ± 1.4
MDA (μmol/mg protein)	1.28 ± 0.32	1.44 ± 0.28	0.95 ± 0.18	1.10 ± 0.3
GSH (ng/mg protein)	114.2 ± 12.5	98.7 ± 9.65	120.7 ± 15.3	113.1 ± 10.4

Note. Values are means ± SE; $n = 2$ of 4 slices.

1972; Terris, 1986) means that data derived from it may be of more direct clinical relevance to humans. Porcine tissue slices have already been reported to respond to other toxins (Fisher *et al.,* 1991).

Precision-cut tissue slices offer the only practical and cost effective means of making such an assessment, which has significant advantages over *in vitro* isolated fragments and conventional cell culture or cocultures (Obatomi and Bach, 1996a,b; Obatomi and Bach, 1997). Slices maintain their normal cellular architecture and cell–cell communication, which more closely represents the *in vivo* situation of tissues and makes the comparison of different organs from several species straightforward. Slices prepared in submersion culture from our laboratory (Obatomi *et al.,* 1997) are viable and maintain cellular and metabolic functions for up to 24 h. Significant toxicological changes were observed in renal fragments as early as 1 h after exposure to ATR (Obatomi and Bach, 1996a,b), and in addition, ultrastructural changes have been shown to occur within 3 h of intraperitoneal administration of ATR (50 mg/kg bw) to rat (Carpenedo *et al.,* 1974) and dogs (Koechel and Krejci, 1993). Thus the exposure of tissue slices reported in this study to ATR for 3 h was used to mirror the acute effects of the toxin.

This study demonstrated differences in the basal biochemistry of untreated kidney and liver slices from the two species. Interference with hepatic and renal intermediary metabolism shows that the known *in vivo* effect of ATR is mirrored in slices and also helps compare the sensitivity of different tissues and species. *In vivo,* ATR is known to affect anabolic processes (Obatomi and Bach, 1997). It induces transient hyperglycemia followed by hypoglycemia, acidosis, and decreased rate of oxygen consumption (Roeder *et al.,* 1994). We have previously shown (Thanh *et al.,* 1997) that ATR also changes lipid metabolism in rat liver and kidney slices. Our present data show an ATR-induced reduction in glucose concentration *in vitro* and a significant inhibition of gluconeogenesis in both liver and kidney, an effect that results in reduction of tissue glucose and consequently an inhibition of one of the key functions of these organs. Inhibition of glucose production in liver slices agrees with previously reported data (Ishii and Bracht, 1986) by using liver perfusion. These results are therefore consistent with the *in vivo* observation since there are similar patterns of metabolic alterations in both liver and kidney. This is not surprising as ATR also caused an ATP depletion, which may be the cause of significant inhibition of gluconeogenesis, a process known to be ATP-dependent. However, the highest concentration of ATR caused no more than a 50% decrease in cellular ATP. Concentrations of ATR that are quite cytotoxic when assessed by enzyme leakage (Figs. 4 and 5) have only a modest effect on cellular ATP. This suggests that cytotoxicity may not be as a result of perturbing cellular energy alone.

The utilization of marker enzymes as indices of cytotoxic damage are widely used in slices (Rankin *et al.,* 1994). The cytosolic marker enzyme LDH is present in all cells, but especially centrilobular liver (Jungermann and Katz, 1989), whereas the membrane bound, brush border enzyme ALP is a regiospecific marker of proximal brush border (Guder and Ross, 1984) and the periportal region of the liver (Jungermann and Katz, 1989). Thus the simultaneous leakage of both LDH and ALP from the kidney, but not liver or the striated muscle (relative to their respective controls), strongly suggests the injury induced by ATR to be site-specific and depends on factors other than the interaction between mitochondria and ATR. Indeed, previous reports have shown ATR to affect the proximal tubule histology *in vivo* (Carpenedo *et al.,* 1974; Bhoola, 1983). This may also be true of the liver in which only LDH was significantly increased following treatment with ATR. Previous histopathological studies also showed specific centrilobular (not periportal) hepatic necrosis following treatment with ATR *in vivo* (Bhoola, 1983). Thus ATR was potently cytotoxic in both rat and porcine renal cortical and hepatic, but not striated muscle slices. The liver and kidney tissue from these two species responded similarly to ATR, but renal slices appeared to be more sensitive than hepatic slices in both species.

ATR impairs oxidative phosphorylation (Allman *et al.,* 1967), which has been assumed to be the mechanism of cellular injury. This simplistic approach does not explain why the proximal tubule (Obatomi and Bach, 1997; Bhoola, 1983) or the centrilobular region of the liver (Georgiou *et al.,* 1988) are selectively injured, nor does it explain other pathophysiologi-

cal changes involved in renal necrosis or fatalities. Both isolated liver and kidney mitochondrial are similarly inhibited by ATR (Obatomi and Bach, 1997), but the results obtained in this study show that mitochondrial toxicity appears to be less prominent in these intact tissues, although the ATP content was significantly altered in both kidney and liver slices and in both species. This alteration was modest at concentrations of ATR that were cytotoxic. The MTT assay, which measures mitochondrial function as a general index of cellular viability (Mosbann, 1978), was less sensitive a cytotoxic marker than other parameters, but this could be explained by recent studies which demonstrated that the assay also measured some extramitochondrial effect (Berridge and Tan, 1993) and by the limited effects of ATR on ATP in slices. While there was significant ATR-related reduction in formazan formation in the kidney, there was little change in the liver. Thus the mitochondrial effects of ATR do not, on their own, account for selective toxicity in higher order systems such as slices. The relative interspecies differences in sensitivity of MTT assay on the one hand, compared to other parameters, also suggest that the cytotoxic effect of ATR does not relate to its mitochondrial effects alone. The concentration-dependent decrease in ATP content of slices also suggests that ATR acts by altering the bioenergetic balance of the cells. The decrease in ATP content may be due to a dramatic increase in the energy demand, which may be caused by ATR or the reduced production of ATP due to the inhibition of the ATP/ADP translocase or both processes.

The role of ATR metabolism in its toxicity is not clear, but ATR does interact with hepatic biotransformation systems (Schnellman and Mandel, 1985). Site- and organ-specific target of ATR reflecting a possible mechanism of action is also reflected by the difference in lipid peroxidation and changes in GSH level following exposure of kidney and liver slices to ATR. Thus the very significant increase in MDA production (twofold in rat and fourfold in pig) in liver, but not in kidney, supports a dose-related lipid peroxidation following ATR exposure.

The present data provide evidence of a dose-dependent GSH depletion in liver and kidney and a significant increase in GSSG level only in the liver. Statistically significant increases in the ratio GSH:GSSG were only observed in liver slices of both species, although this was more pronounced in the pig tissue. This invariably suggests that while ATR nephrotoxicity involves only the depletion of cellular GSH, hepatotoxicity is accompanied by both lipid peroxidation and GSH depletion. The liver may therefore be a major site for oxidative stress *in vivo* as ATR did not induce lipid peroxidation in the kidney slices from either rats or pigs. This is supported by data from rat renal fragments exposed to ATR (Obatomi and Bach, 1996a). The presence of a methylene moiety in ATR (Fig. 1) suggests the possibility of free radical formation, especially as the presence of an oxidized ATR metabolite has been detected in urine (Obermann *et al.,* 1973). Since lipid peroxidation destroys biological membranes, it is reasonable to suggest this would result in hepatic damage, disturbed liver function, and cell necrosis. Such an effect may explain why significant LDH but not ALP leakage occurs from liver slices of both species. The reactive intermediate that underlies ATR-induced lipid peroxidation has not been identified, but reactive oxygen species such as superoxide anion, hydrogen peroxide, or hydroxyl radicals may be involved (Slater, 1984). The extent of lipid peroxidation appeared to correlate with the extent of injury and was dose related. Since the GSH pools within the kidney are highly concentrated in the proximal tubule (Schnellman and Mandel, 1985), it will be reasonable to suggest that this region was mostly affected, especially as the release of LDH and ALP reported here directly identifies this region to be susceptible. The lack of significant increase in GSH:GSSG ratio in kidney slices suggests that some GSH may be conjugated with an active metabolite of ATR or the presence of this diterpenoid reduced *de novo* GSH synthesis. Lipid peroxidation and/or GSH depletion following ATR exposure was limited to kidney and liver, but there were no changes in striated muscle, which suggests that it represents a nontarget tissue.

There is a paucity of data on ATR transport, excretion, and biotransformations as assumptions are usually made when the compound is used in investigations concerning control of metabolic fluxes. ATR is significantly excreted in urine of exposed animals (Bye, 1991); thus the kidney is probably a major site of excretion, where ATR may accumulate by selective uptake. The presence of a sulphated glycoside, with an aglycone moiety of ATR (Fig. 1), makes this molecule a candidate for anion transport (Luciani *et al.,* 1978; Koechel and Krejci, 1993). The importance of anion transport is supported as probenecid pretreatment apparently delays the onset of nephrotoxicity in spontaneously respiring dogs (Koechel and Krejci, 1993). Our data show that ATR inhibits PAH uptake in a dose- and time-dependent manner, which may be explained by a common transport mechanism. Taken together these observations lend strength to the hypothesis (Obatomi and Bach, 1996a,b, 1997) that the preferential uptake and renal accumulation of free ATR may explain the site selectivity and sensitivity of its toxicity. This also offers a rational approach to modulating the effects of the compound in poisoned humans. Similarly, evidence of oxidative stress and GSH depletion suggests that the administration of antioxidants may be therapeutically useful.

In summary, we have assessed the toxicity of ATR in rat and pig renal and liver tissue slices compared to striated muscle slices. No evidence of toxicity was observed in the striated muscle slices. Both the kidney and liver slices from the rat and the pig showed similar responses to ATR in relation to cytotoxicity, and changes in metabolic and energy balance. The

basic mechanisms of toxicity in the two organs appear to be different. Our data show an interaction between PAH and ATR in the kidney and a depletion of GSH, while in the liver, toxicity is accompanied by both GSH depletion, a significant decrease in GSH:GSSG ratio, and an increase in lipid peroxidation. ATR toxicity in liver may be caused by oxidative stress. This is not the case for the proximal tubule, where a reduction in *de novo* GSH synthesis or ATR conjugation could occur, especially as this molecule may be accumulated by the anion transport system. There were interspecies and organ differences in some baseline biochemical data, but this was not responsible for different responses to ATR toxicity. Mitochondrial function using MTT was the least sensitive measure of cytotoxicity and does not appear to be a very useful parameter for the short-term effects of ATR in slices.

ACKNOWLEDGMENTS

This work was supported by funding from Higher Education Funding Council of England and in part by the British Council. D.K.O. is a visiting Research Fellow. We acknowledge Dr. Robyn Fisher for her useful comments.

REFERENCES

Allman, D. W., Harris, R. A., and Green, D. (1967). Site of action of atractyloside in mitochondria II. Inhibition of oxidative phosphorylation. *Arch. Biochem. Biophys.* **122,** 766–782.

Bach, P. H., Obatomi, D. K., and Brant, S. (1996a). In vitro models for nephrotoxicity screening and risk assessment. In *In Vitro Methods in Pharmaceutical Research* (J. V. Castell and M. J. Gomez-Lechon, Eds.), pp. 55–101. Academic Press, London.

Bach, P. H., Vickers, A. E. M., Fisher, R., Baumann, H., Brittebo, E., Carlile, D. J., Koster, H. J., Lake, B. G., Salmon, F., Sawyer, T. W., and Skibinski, G. (1996b). The use of tissue slices for pharmacotoxicology studies. The report and recommendations of ECVAM workshop. *ATLA* **24,** 893–923.

Berridge, M. V., and Tan, A. S. (1993). Characterization of the cellular reduction of 3-(4,5-dimethylthiazol-2-yl)-2,5-diphenyltetrazolium bromide (MTT) subcellular localisation, substrate dependence and involvement of mitochondrial electron transport in MTT reduction. *Arch. Biochem. Biophys.* **303,** 474–482.

Bhoola, K. D. N. (1983). *A Clinico-pathological and Biochemical Study of Callilepsis laureola* (impila). Doctor of Medicine Thesis, University of Natal, Durban.

Brendel, K., Fisher, R. L., Krumdieck, C. L., and Gandolfi, A. J. (1993). Precision-cut liver slices in dynamic organ culture for structure-toxicity studies. In *In Vitro Biological Systems, Vol. 1.* (C. A. Tyson and J. M. Frazier, Eds.), pp. 222–230. Academic Press, San Diego.

Burge, J. A., and Aust, S. D. (1978). Microsomal lipid peroxidation. *Meth. Enzymol.* **52,** 302–310.

Bye, S. N. (1991). *The Development of Assays for Atractyloside and Its Localisation in Rat Tissue.* Doctor of Philosophy Thesis, University of Natal, Pietermantzburg.

Caravaca-Magarinos, F., Cubero-Gomez, J. J., and Arrobasvaca, M. (1985). Renal and hepatic injuries in human intoxication with *Atractylis gummifera. Nefrologia* **5,** 205–210.

Carpenedo, F., Luciani, S., Scaravilli, F., Palatine, P., and Santi, R. (1974). Nephrotoxic effect of atractyloside in rats. *Arch. Toxicol.* **32,** 169–180.

DeLuca, M., and McElroy, N. D. (1978). Purification and properties of firefly luciferase. *Meth. Enzymol.* **57,** 3–14.

Douglas, W. R. (1972). Of pigs and men and research: A review of applications and analogies of the pig in human medical research. *Space Life Sci.* **3,** 226–234.

Edindin, M. (1970). A rapid quantitative fluorescence assay for cell damage by cytotoxic antibodies. *J. Immunol.* **104,** 1303–1306.

Fisher, R. L., Sipes, I. G., Gandolfi, A. J., and Brendel, K. (1991). Cryopreservation of pig and human liver slices. *Cryobiology* **28,** 131–142.

Fujimoto, Y., and Fujita, T. (1982). Effect of lipid peroxidation on p-aminohippurate transport by rat kidney cortical slices. *Br. J. Pharmacol.* **786,** 373–379.

Gandolfi, A. J., Brendel, K., and Fernando, Q. (1996). Preparation and use of precision-cut renal cortical slices in renal toxicology. In *Methods in Renal Toxicology* (R. K. Zalups and L.H. Lash, Eds.), pp. 100–122. CRC Press, Boca Raton, FL.

Georgiou, M., Sianidon, L., Hatzis, T., Papadatos, J., and Kouselini, S. A. (1988). Hepatotoxicity due to *Atractylis gummifera L. Clin. Toxicol.* **26,** 487–493.

Guder, W. G., and Ross, B. D. (1984) Enzyme distribution along the nephron. *Kidney Int.* **26,** 101–111.

Hissin, P. J., and Hilf, R. (1976). A fluorometric method for determination of oxidized and reduced glutathione in tissues. *Anal. Biochem.* **74,** 214–226.

Hutchings, A., and Terblanche, S. E. (1989). Observation on the use of some known and suspected toxic Liliflorae in Zulu and Xhosa medicine. *S. Afr. Med. J.* **75,** 62–69.

Ishii, E. L., and Bracht, A. (1986). Stevioside, the sweet glycoside of *Stevia rebaudina* inhibits the action of ATR in the isolated perfused rat liver. *Res. Commun. Chem. Path. Pharmacol.* **53,** 79–97.

Jungermann, K., and Katz, N. (1989) Functional specialisation of different hepatocyte populations. *Physiol. Rev.* **69,** 708–764.

Koechel, D. A., and Krejci, M. E. (1993). Extrarenal and direct anaesthesized actions of atractyloside contributes to its acute nephrotoxicity in pentobarbital dogs. *Toxicology* **79,** 45–66.

Krumdieck, C. L., dos Santos, J. E., and Ho, K. J. (1980). A new instrument for the rapid preparation of tissue slices. *Anal. Biochem.* **104,** 118–123.

Luciani, S., Carpenedo, F., and Tarjan, E. M. (1978). Effects of atractyloside and carboxy-atractyloside in the whole animal. In *Atractyloside, Chemistry, Biochemistry and Toxicology* (R. Santi and S. Luciani, Eds.), pp. 109–124. Picin, Padova, Italy.

Mosbann, T. (1978). Rapid colorimetric assay for cellular growth and survival: application to proliferation and cytotoxicity assays. *J. Immunol. Meth.* **65,** 55–63.

Mount, L. E., and Ingram, D. L. (1971). *The Pig as a Laboratory Animal.* Academic Press, London.

Obatomi, D. K., and Bach, P. H. (1996a). Selective cytotoxicity associated with in vitro exposure of fresh rat renal fragments and continuous cell lines to atractyloside. *Arch. Toxicol.* **71,** 93–98.

Obatomi, D. K., and Bach, P. H. (1996b). Inhibition of mitochondrial respiration and oxygen uptake in isolated renal tubular fragments by atractyloside. *Toxicol. Lett.* **89,** 155-161.

Obatomi, D. K., and Bach, P. H. (1997). Biochemistry and toxicology of the diterpenoid glycoside atractyloside. *Fd. Chem. Toxicol.,* in press.

Obatomi, D. K., and Plummer, D. T. (1995). Renal damage caused by gentamicin: a study of the effect using isolated proximal tubular fragments. *Toxicol. Lett.* **75,** 75–83.

Obatomi, D. K., Brant, S., Kaler, S., Anthonypillai, V., and Bach, P. H. (1997). Reduced susceptibility of renal slices to oxidative damage. *Biochem. Soc. Trans.* **25,** 36S.

Obermann, H., Spiteller, G., and Hayer, G. A. (1973). Struktureines aus menschenharn isolierten C19-Terpenoids-2β-hydroxy-15-oxoatractylan-4α-carbonsaure. *Chem. Ber.* **106,** 3506–3518.

Plummer, D. T. (1987). *An Introduction to Practical Biochemistry*, 3rd Ed. McGraw-Hill, London.

Rankin, G. O., Valentovic, M. A., Nicoll, D. W., Ball, J. G., Anestis, D. K., Wang, R. T., and Brown, P. I. (1994). In vivo and in vitro 4-amino-2,6-dichlorophenol nephrotoxicity and hepatotoxicity in the Fischer 344 rat. *Toxicology* **90,** 115–128.

Read, S. M., and Northcote, D. H. (1981). Minimization of variation in the response to different proteins of the Coomassie Blue G-dye binding assay for protein. *Anal. Biochem.* **116,** 53–59.

Roeder, E., Bouramel, T., Meier, U., and Wiedenfeld, H. (1994). Diterpenoid glycosides from *Iphioma aucheri. Phytochemistry* **37,** 353–355.

Roobol, A., and Alleyne, G. A. O. (1974). Control of renal cortex: Ammoniagenesis and its relationship to renal cortex gluconeogenesis. *Biochim. Biophys. Acta* **362,** 83–88.

Schnellman, R. G., and Mandel, L. J. (1985). Intracellular compartmentation of glutathione in rabbit renal proximal tubule. *Biochem. Biophys. Res. Commun.* **133,** 1001–1005.

Schteingart, C. D., and Pomilio, A. B. (1984). Atractyloside, toxic compound from *Wedelia glauca. J. Natural Prod. (Llyodia)* **47,** 1046–1047.

Slater, F. F. (1984). Free radical mechanisms in tissue injury. *Biochem. J.* **122,** 1–15.

Smith, H. W., Finkelsteine, N., Aliminosa, L., Crawford, B., and Graber, M. (1944). The renal clearances in dog and man. *J. Clin. Invest.* **24,** 388–404.

Terris, J. M. (1986). Swine as a model in renal physiology and nephrology: an overview. In *Swine in Biomedical Research* (M. E. Tumbleson, Ed.), pp. 1673–1680. Plenum, New York.

Thanh, N. T. K., Obatomi, D. K., and Bach, P. H. (1997). Lipid profiling in renal and hepatic tissue slices following exposure to atractyloside. *Biochem. Soc. Trans.* **25,** 35S.

Wainwright, J., Scholand, M. M., and Candy, H. (1977). Toxic hepatitis in Black patients in Natal. *S. Afr. Med. J.* **51,** 571–573.